

# Control of multipolar and orbital order in perovskite-like $[\text{C}(\text{NH}_2)_3]\text{Cu}_x\text{Cd}_{1-x}(\text{HCOO})_3$ metal–organic frameworks

Nicole L. Evans,<sup>a</sup> Peter M. M. Thygesen,<sup>a</sup> Hanna L. B. Boström,<sup>a</sup> Emily M. Reynolds,<sup>a</sup> Ines E. Collings,<sup>b</sup> Anthony E. Phillips,<sup>c</sup> and Andrew L. Goodwin<sup>a\*</sup>

<sup>a</sup>Department of Chemistry, University of Oxford, Inorganic Chemistry Laboratory, South Parks Road, Oxford OX1 3QR, U.K.

<sup>b</sup>Laboratory of Crystallography, University of Bayreuth, D-95440 Bayreuth, Germany

<sup>c</sup>School of Physics and Astronomy, Queen Mary, University of London, 327 Mile End Road, London E1 4NS, U.K.

## Supporting Information Available

**ABSTRACT:** We study the compositional dependence of molecular orientation (multipolar) and orbital (quadrupolar) order in the family of perovskite-like metal–organic frameworks  $[\text{C}(\text{NH}_2)_3]\text{Cu}_x\text{Cd}_{1-x}(\text{HCOO})_3$ . On increasing the fraction  $x$  of Jahn-Teller-active  $\text{Cu}^{2+}$ , we observe first an orbital disorder/order transition and then a multipolar reorientation transition, each occurring at distinct critical compositions  $x_o = 0.45(5)$  and  $x_m = 0.55(5)$ . We attribute these transitions to a combination of size, charge distribution, and percolation effects. The transitions we observe establish the accessibility in formate perovskites of novel structural degrees of freedom beyond the familiar dipolar terms responsible for (anti)ferroelectric order. We discuss the symmetry implications of cooperative quadrupolar and multipolar states for the design of relaxor-like hybrid perovskites.

Some of the most important and interesting phenomena exhibited by conventional oxide perovskites arise from the coupling of ostensibly independent degrees of freedom.<sup>1,2</sup> In the colossal magnetoresistance (CMR) manganites, for example, it is an interplay between charge localization, magnetic order, orbital order, and atom displacements that allows conductivity to be switched on and off in response to external magnetic fields.<sup>3–5</sup> Likewise, the anomalous dielectric behavior of relaxor ferroelectrics arises from coupling of compositional variation with orbital and dipole orientations.<sup>6</sup>

Over the past 5–10 years it has become obvious that many of these same degrees of freedom are as relevant to metal–organic frameworks (MOFs) and hybrid inorganic/organic solids as they are to conventional oxide ceramics.<sup>7,8</sup> It is this realization that has fuelled the quest for multiferroic MOFs, for example, where coupled

magnetic spin and dipolar order would allow magnetic-field switching of bulk polarization—an attractive property in device component design.<sup>9–14</sup> The relevance to photovoltaic performance in hybrid organic perovskites has also become increasingly clear: anomalous exciton lifetimes in these systems are now understood to emerge from a complex interplay between cooperative molecular tumbling, lattice vibrations, and polar displacements.<sup>15–17</sup>

In this context, the MOF community has focused almost exclusively on the cooperative behavior of *dipolar* degrees of freedom (e.g. molecular dipole orientations,<sup>18–20</sup> ion displacements,<sup>21</sup> magnetic order<sup>21–24</sup>), presumably because these are directly susceptible to external fields. Yet MOFs also allow access to a variety of quadrupolar and higher-order multipolar ordering processes, the phenomenology of which is almost entirely unexplored.<sup>25,26</sup> For example, the charge distribution of guanidinium (point symmetry  $D_{3h}$ ) is multipolar rather than dipolar [Fig. 1(a)],<sup>27</sup> and so molecular orientations in guanidinium-containing MOFs can actually be described by different states of multipolar order.<sup>26</sup> These states will be conceptually related to the “hidden order” phases<sup>28,29</sup> of  $\text{URu}_2\text{Si}_2$  and  $\text{Ga}_3\text{Gd}_5\text{O}_{12}$  and often have no direct analogue in conventional oxide perovskites. A related phenomenon is the quadrupolar order associated with cooperative Jahn Teller distortions observed in e.g.  $[\text{A}]\text{Cu}(\text{HCOO})_3$  hybrid frameworks (here  $\text{A}^+$  is a molecular cation).<sup>30,31</sup> An extremely important result of Ref. 9 was to demonstrate that this quadrupolar order in guanidinium copper formate could itself induce a macroscopic dipole, allowing indirect design of polar states in a similar manner to the “tilt engineering” approach recently developed for perovskites.<sup>32</sup> So while these more complex degrees of freedom accessible to MOFs may not be directly susceptible to manipulation by external fields

they can nevertheless couple to degrees of freedom that are susceptible. Hence there is substantial unrealized potential for developing new functional MOFs based on exploiting ordering behavior of complex degrees of freedom.

It was in this context that we chose to study the phase behavior of the hybrid perovskite analogues  $[\text{C}(\text{NH}_2)_3]\text{Cu}_x\text{Cd}_{1-x}(\text{HCOO})_3$ . Relatively few mixed-metal formates appear to have been reported elsewhere,<sup>33–35</sup> and here only the  $x = 0$  and 1 end-members have been characterized previously.<sup>30,36</sup> They adopt structures with different guanidinium arrangements, and so are related to different states of multipolar order. Whereas in the Cd compound the molecular  $C_3$  axes align along a single  $[111]$ -type direction of the underlying cubic net (we refer to this arrangement as ‘R-type’ as it enforces rhombohedral symmetry), in the Cu compound alignment is along an alternating pair of  $\langle 111 \rangle$  directions to give a structure with orthorhombic symmetry (hence ‘O-type’) [Fig. 1(b)]. Both arrangements are mediated by hydrogen-bonding interactions between the guanidinium cation and formate linkers of the anionic host framework.<sup>30</sup> In the absence of further symmetry-breaking distortions, the R and O multipole states are described by the space groups  $R\bar{3}c$  and  $Pnna$ , respectively.<sup>37</sup> The lower symmetry of the Cu compound observed experimentally ( $Pna2_1$ , a polar space group) arises from coexistence of O-type multipole order with the quadrupolar orbital order of its cooperative Jahn-Teller (JT) distortion.<sup>9</sup> Combining the same orbital arrangement with the R multipole state results in the centrosymmetric space-group  $P2_1/c$  (see SI). Hence polarization is a non-trivial consequence of the symmetries of quadrupolar and multipolar order [Fig. 1(c)].<sup>9,10</sup> By studying the solid solution between the Cd and Cu end-members, we determine the extent to which the multipolar and quadrupolar order jointly responsible for bulk polarization in  $[\text{C}(\text{NH}_2)_3]\text{Cu}(\text{HCOO})_3$  might be controlled independently of one another, and hence exploited in future materials design.

Using the approach developed in Refs. 24 and 36 we prepared polycrystalline samples of  $[\text{C}(\text{NH}_2)_3]\text{Cu}_x\text{Cd}_{1-x}(\text{HCOO})_3$  with  $x = 0, 0.1, 0.2, \dots, 1$ ; compositions were verified using atomic absorption spectroscopy (see SI). High-resolution synchrotron X-ray diffraction patterns measured for these compounds show a progressive shift in peak positions and diffraction profiles that is consistent with solid solution formation across the entire composition field [Fig. 2(a)]. Two clear transitions are observed, dividing the phase field into three regions. The first occurs for the most Cu-poor samples ( $0 \leq x \leq 0.4$ ): here the structure type is that of the Cd parent ( $R\bar{3}c$ ), indicating R-type multipole order and the expected absence of quadrupolar JT order. The second is observed for the single composition  $x = 0.5$ . Here the diffraction pattern can be accounted for by a single phase of sym-

metry  $P2_1/c$ , which is consistent with a combination of R multipole order and quadrupolar order from cooperative JT distortions. The existence of a monoclinic distortion is clearly evident in the splitting of relevant reflections [see inset to Fig. 2(a)]; this splitting cannot be as convincingly accounted for by a two-phase ( $R\bar{3}c + Pna2_1$ ) model (see SI). The third and final region occurs for  $0.6 \leq x \leq 1$ , where it is the  $Pna2_1$  phase of the Cu end-member that is stable. The crystal symmetry of this phase is consistent with the combination of O-type multipolar order and the same quadrupolar orbital order observed in the Cu end-member itself. At no point did we observe any evidence for cation ordering (despite the sensitivity one would expect with X-rays were such order to occur); the crystal symmetries of each phase are consistent only with a single Cd/Cu crystallographic site. Consequently we attribute the transitions at  $x_0 = 0.45(5)$  and  $x_m = 0.55(5)$ , respectively, to orbital order and multipole reorientation transitions. To the best of our knowledge, this is the first identification of these classes of transitions in a MOF/hybrid system.

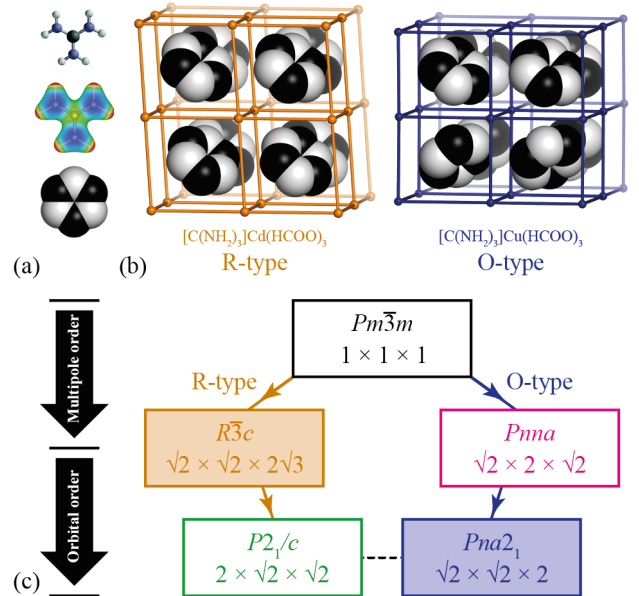


Figure 1. (a) Guanidinium ion (top), electrostatic potential (middle) and multipolar representation (bottom). (b) Multipole order in Cd- (left) and Cu-containing (right) guanidinium formates; metal-formate linkages are represented by straight rods for clarity. (c) Symmetry relationships between multipolar and orbital ordering processes as described in the text. Arrows represent group-subgroup relationships; the dashed line represents a discontinuous pathway. Experimentally-observed<sup>30,36</sup> space-groups for the Cd (orange) and Cu (blue) formate perovskites are shaded.

The variation in lattice parameters as a function of  $x$  was determined using Pawley refinement [Fig. 2(b)] (see SI). Within a given phase the variation is smooth, supporting the assertion that we have prepared a genuine solid solution. However, both transitions appear discontinuous and are accompanied by volume anomalies. The

volume *increase* with orbital order at  $x_0$  is not without precedent: a similar effect is observed in  $\text{LaMnO}_3$  at its thermally-driven orbital order/disorder transition.<sup>38,39</sup> We note that the different signs of the  $\Delta V$  term associated with orbital and multipolar ordering suggests that pressure may be used as a variable to manipulate these transitions independently of one another.

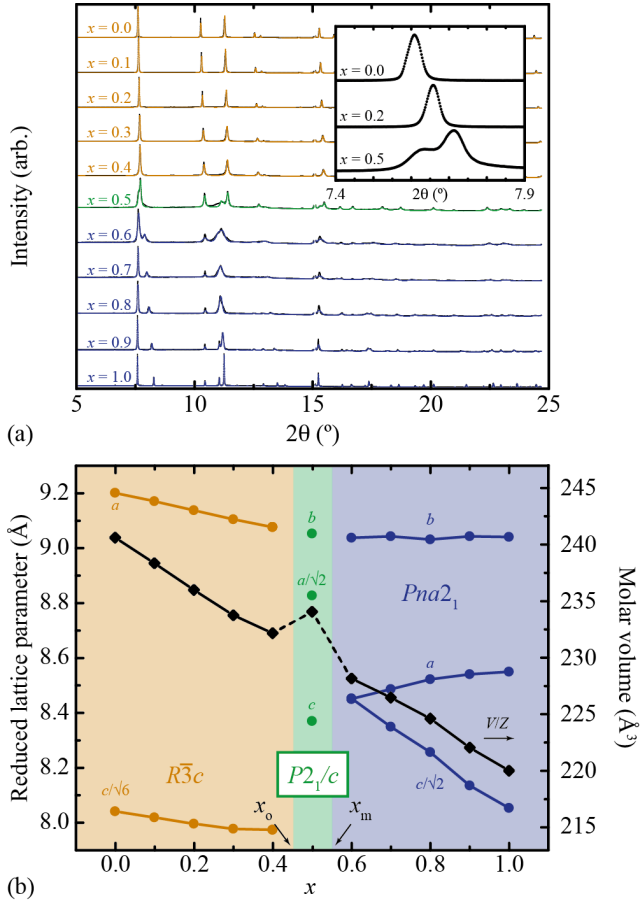


Figure 2. (a) Synchrotron X-ray diffraction patterns ( $\lambda = 0.82599(1) \text{ \AA}$ ) for  $[\text{C}(\text{NH}_2)_3]\text{Cu}_x\text{Cd}_{1-x}(\text{HCOO})_3$ . The inset shows the splitting of a single reflection on transition from  $R\bar{3}c$  ( $x \leq 0.4$ ) to  $P2_1/c$  ( $x = 0.5$ ). (b) Corresponding lattice parameters, determined using Pawley refinement.

So how might we understand the microscopic mechanisms responsible for transitions at  $x_0$  and  $x_m$ ? We suggest there are three key effects associated with increasing Cu composition.

First is that of size: the difference in Cu–O and Cd–O bond lengths (2.1 and 2.3  $\text{\AA}$ , respectively<sup>30,36</sup>) means that the edge length of the cubic perovskite net is somewhat shorter in  $[\text{C}(\text{NH}_2)_3]\text{Cu}(\text{HCOO})_3$  than in  $[\text{C}(\text{NH}_2)_3]\text{Cd}(\text{HCOO})_3$ : 6.03 vs 6.24  $\text{\AA}$ . This comparison holds not only for Cu but for all the first-row transition-metals; that the analogous framework for each of these systems adopts the same O multipole state<sup>30</sup> suggests this particular arrangement of guanidinium cations may simply reflect a more efficient packing. In other words, the reduction in molar volume on Cu doping [Fig. 2(b)]

may drive the multipole state transition in order to pack guanidinium ions more efficiently.

A second, albeit related, factor is the variation in strength of hydrogen bonding interaction between guanidinium and host framework induced as the transition-metal is varied.<sup>36,40–42</sup> One expects R and O multipole states to support different cation–framework interaction strengths,<sup>41,42</sup> suggesting that a change in charge density may also explain the transition at  $x_m$ .

The final effect we consider is that of introducing JT-active ions into a JT-inactive matrix. On one level, it is perhaps surprising that even in flexible MOFs the local strains associated with JT distortions are sufficient to enforce coupling between orbital orientations of neighboring cations. Yet orbital order is indisputably present in the crystal structure of  $[\text{C}(\text{NH}_2)_3]\text{Cu}(\text{HCOO})_3$  itself.<sup>30</sup> For small values of  $x$ , the JT axes of isolated  $\text{Cu}^{2+}$  ions will be uncorrelated since most ions are surrounded by a JT-inactive matrix of  $\text{Cd}^{2+}$ . As  $x$  increases, however, the fraction of  $\text{Cu}^{2+}$  ions with  $\text{Cu}^{2+}$  neighbors will quickly increase, and strain effects will enforce local coupling between their orbital orientations. At some critical Cu composition these correlations will become long-range, resulting in an orbital disorder/order transition; on the basis of symmetry arguments we identify this as the transition at  $x_0$ . We used a simple Monte Carlo (MC) simulation to identify the composition at which this transition might be expected to occur (see SI). Our toy Hamiltonian considers the effect of random-site percolation on a cubic lattice taking into account only nearest-neighbor interactions. For this model, we find that the orbital order phase transition occurs at  $x_0 \sim 0.6$ . That orbital order sets in at a lower value of  $x$  in the experimental system suggests (i) the existence of short-range cation order and/or (ii) the JT strain field is meaningfully longer-range than nearest-neighbor interactions.<sup>43</sup>

As further checks we investigated the temperature dependence of the transitions at  $x_0$  and  $x_m$  (there is none, consistent with percolative mechanisms;<sup>44</sup> see SI) and also established the corresponding phase behavior of the solid solution  $[\text{C}(\text{NH}_2)_3]\text{Mn}_x\text{Cd}_{1-x}(\text{HCOO})_3$ . In this Mn-containing system both cations are JT inactive, and we now observe a single, temperature-dependent, multipole transition from  $R\bar{3}c$  directly to  $Pnna$  [Fig. 1(c)] (see SI). This transition occurs at a higher doping level  $x_m(\text{Mn}) = 0.75(5)$ , which is consistent with the size arguments presented above.<sup>45</sup>

So we have demonstrated for a family of perovskite-like MOFs that multipolar and orbital degrees of freedom undergo independent ordering processes as a result of compositional variation. The particular system we study here has a readily identifiable signature of orbital order (rhombohedral–monoclinic splitting). However, one expects similar phenomena in families such as  $[\text{C}(\text{NH}_2)_3]\text{Cu}_x\text{Mn}_{1-x}(\text{HCOO})_3$ , where the emergence of weak forbidden reflections would identify progression

from disordered ( $Pnna$ ) to ordered ( $Pna2_1$ ) states. Compositions in the vicinity of this transition may prove especially interesting since the symmetry arguments of Ref. 9 guarantee that critical fluctuations in orbital order must couple to fluctuations in the polarization to give polar nano-domain structures more usually associated with the Pb-containing perovskite relaxors PZN/PMN.<sup>46</sup> Not only do our results suggest an avenue for the design of lead-free relaxors, but the inclusion of magnetic transition metals such as  $Mn^{2+}$  and  $Cu^{2+}$  allows in principle for subsequent coupling to magnetic order. Moreover, since different organic cations have different multipolar charge distributions, substitution of this component<sup>47,48</sup> is an obvious means of exploring a large variety of multipolar states. In all cases both the statistical mechanics and the symmetry implications of correlated multipolar, quadrupolar, and dipolar order will prove crucial in exploiting the degrees of freedom accessible to MOFs.

## ASSOCIATED CONTENT

**Supporting Information.** The Supporting Information is available free of charge on the ACS Publications website. Experimental methods; powder diffraction refinement details; lattice parameters; Monte Carlo simulation description; symmetry discussion (PDF).

## AUTHOR INFORMATION

### Corresponding Author

andrew.goodwin@chem.ox.ac.uk

### Funding Sources

No competing financial interests have been declared.

European Research Council (Grant 279705).

This project has received funding from the European Union (EU) Horizon 2020 research and innovation programme under the Marie Skłodowska-Curie grant agreement number 641887 (project acronym DEFNET).

## ACKNOWLEDGMENT

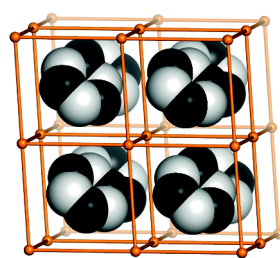
The authors gratefully acknowledge useful discussions with J. A. Hill (Oxford). The synchrotron diffraction measurements were carried out at the Diamond Light Source (I11 Beamline). We are extremely grateful for the award of a Block Allocation Grant, which made this work possible, and for the assistance in data collection provided by M. S. Senn (Oxford) and the I11 beamline staff.

## REFERENCES

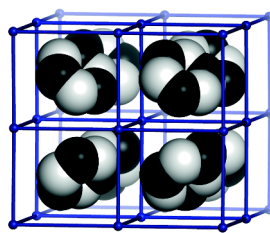
- (1) Lee, J. H.; Fang, L.; Vlahos, E.; Ke, X.; Jung, Y. W.; Kourkoutis, L. F.; Kim, J.-W.; Ryan, P. J.; Heeg, T.; Roeckerath, M.; Goian, V.; Bernhagen, M.; Uecker, R.; Hammel, P. C.; Rabe, K. M.; Kamba, S.; Schubert, J.; Freeland, J. W.; Muller, D. A.; Fennie, C. J.; Schiffer, P.; Gopalan, V.; Johnston-Halperin, E.; Schlom, D. G. *Nature* **2010**, *466*, 954-959.
- (2) Millis, A. J. *Nature* **1998**, *392*, 147-150.
- (3) Jin, S. *Science* **1994**, *264*, 413-415.
- (4) Goodenough, J. B., *Phys. Rev.* **1955**, *100*, 564-573.
- (5) Adams, C. P., *Phys. Rev. Lett.* **2000**, *85*, 3954-3957.

- (6) Xu, G.; Zhong, Z.; Bing, Y.; Ye, Z.-G.; Shirane, G., *Nat. Mater.* **2006**, *5*, 134-140.
- (7) Jain, P.; Dalal, N. S.; Toby, B. H.; Kroto, H. W.; Cheetham, A. K., *J. Am. Chem. Soc.* **2008**, *130*, 10450-10451.
- (8) Rogez, G.; Viart, N.; Drillon, M. *Angew. Chem. Int. Ed.* **2010**, *49*, 1921-1923.
- (9) Stroppa, A.; Jain, P.; Barone, P.; Marsman, M.; Perez-Mato, J. M.; Cheetham, A. K.; Kroto, H. W.; Picozzi, S., *Angew. Chem.* **2011**, *50*, 5847-5850.
- (10) Stroppa, A.; Barone, P.; Jain, P.; Perez-Mato, J. M.; Picozzi, S., *Adv. Mater.* **2013**, *25*, 2284-2290.
- (11) Wang, W.; Yan, L.-Q.; Cong, J.-Z.; Zhao, Y.-L.; Wang, F.; Shen, S.-P.; Zou, T.; Zhang, D.; Wang, S.-G.; Han, X.-F.; Sun, Y., *Sci. Rep.* **2013**, *3*, 2024.
- (12) Tian, Y.; Stroppa, A.; Chai, Y.; Yan, L.; Wang, S.; Barone, P.; Picozzi, S.; Sun, Y., *Sci. Rep.* **2014**, *4*, 6062.
- (13) Jain, P.; Ramachandran, V.; Clark, R. J.; Zhou, H. D.; Toby, B. H.; Dalal, N. S.; Kroto, H. W.; Cheetham, A. K., *J. Am. Chem. Soc.* **2009**, *131*, 13625-13627.
- (14) Gómez-Aguirre, L. C.; Pato-Doldán, B.; Castro-García, S.; Señaris-Rodríguez, M. A.; Sánchez-Andújar, M.; Singleton, J.; Zapf, V. S., *J. Am. Chem. Soc.* **2016**, *138*, 1122-1125.
- (15) Lee, J.-H.; Bristowe, N. C.; Bristowe, P. D.; Cheetham, A. K., *Chem. Commun.* **2015**, *51*, 6434-6437.
- (16) Frost, J. M.; Walsh, A., *Acc. Chem. Res.* **2016**, *49*, 528-535.
- (17) Leguy, A. M. A.; Frost, J. M.; McMahon, A. P.; Sakai, V. G.; Kockelmann, W.; Law, C.; Li, X.; Foglia, F.; Walsh, A.; O'Regan, B. C.; Nelson, J.; Cabral, J. T.; Barnes, P. R. F., *Nat. Commun.* **2015**, *6*, 7124.
- (18) Sánchez-Andújar, M.; Presedo, S.; Yáñez-Vilar, S.; Castro-García, S.; Shamir, J.; Señaris-Rodríguez, M. A., *Inorg. Chem.* **2010**, *49*, 1510-1516.
- (19) Besara, T.; Jain, P.; Dalal, N. S.; Kuhns, P. L.; Reyes, A. P.; Kroto, H. W.; Cheetham, A. K., *Proc. Natl. Acad. Sci., U.S.A.* **2011**, *108*, 6828-6832.
- (20) Mączka, M.; Costa, N. L. M.; Gagor, A.; Paraguassu, W.; Sieradzki, A.; Hanuza, J., *Phys. Chem. Chem. Phys.* **2016**, *18*, 13993-14000.
- (21) Xu, G.-C.; Zhang, W.; Ma, X.-M.; Chen, Y.-H.; Zhang, L.; Cai, H.-L.; Wang, Z.-M.; Xiong, R.-G.; Gao, S., *J. Am. Chem. Soc.* **2011**, *133*, 14948-14951.
- (22) Saines, P. J.; Tan, J.-C.; Yeung, H. H.-M.; Barton, P. T.; Cheetham, A. K., *Dalton Trans.* **2012**, *41*, 8585-8593.
- (23) Saines, P. J.; Paddison, J. A. M.; Thygesen, P. M. M.; Tucker, M. G., *Mater. Horiz.* **2015**, *2*, 528-535.
- (24) Wang, Z.; Zhang, B.; Otsuka, T.; Inoue, K.; Kobayashi, H.; Kurmoo, M., *Dalton Trans.* **2004**, 2209-2216.
- (25) Li, W.; Zhang, Z.; Bithell, E. G.; Batsanov, A. S.; Barton, P. T.; Saines, P. J.; Jain, P.; Howard, C. J.; Carpenter, M. A.; Cheetham, A. K., *Acta Mater.* **2013**, *61*, 4928-4938.
- (26) Hill, J. A.; Thompson, A. L.; Goodwin, A. L., *J. Am. Chem. Soc.* **2016**, *138*, 5886-5896.
- (27) Davis, M. R.; Dougherty, D. A., *Phys. Chem. Chem. Phys.* **2015**, *17*, 29262-29270.
- (28) Mydosh, J. A.; Oppeneer, P. M., *Rev. Mod. Phys.* **2011**, *83*, 1301-1322.
- (29) Paddison, J. A. M.; Jacobsen, H.; Petrenko, O. A.; Fernández-Díaz, M. T.; Deen, P. P.; Goodwin, A. L., *Science* **2015**, *350*, 179-181.
- (30) Hu, K.-L.; Kurmoo, M.; Wang, Z.; Gao, S., *Chem.-Eur. J.* **2009**, *15*, 12050-12064.
- (31) Wang, B.-Q.; Yan, H.-B.; Huang, Z.-Q.; Zhang, Z., *Acta Cryst. C* **2013**, *69*, 616-619.
- (32) Pitcher, M. J.; Mandal, P.; Dyer, M. S.; Alaria, J.; Borisov, P.; Niu, H.; Claridge, J. B.; Rosseinsky, M. J., *Science* **2015**, *347*, 420-424.
- (33) Shang, R.; Sun, X.; Wang, Z.-M.; Gao, S., *Chem. Asian J.* **2012**, *7*, 1697-1707.
- (34) Mączka, M.; Sieradzki, A.; Bondzior, B.; Deren, P.; Hanuza, J.; Hermanowicz, K., *J. Mater. Chem. C* **2015**, *3*, 9337-9345.

- (35) Mączka, M.; Gagor, A.; Hermanowicz, K.; Sieradzki, A.; Macalik, L.; Pikul, A., *J. Solid State Chem.* **2016**, *237*, 150-158.
- (36) Collings I. E.; Hill, J. A.; Cairns, A. B.; Cooper, R. I.; Thompson, A. L.; Parker, J. E.; Tang, C. C.; Goodwin, A. L., *Dalton Trans.* **2016**, *45*, 4169-4178.
- (37) We note that the tilt systems active in both compounds correspond to symmetries that are supergroups of the symmetries arising from multipolar order, allowing multipole-tilt coupling.
- (38) Chatterji, T.; Fauth, F.; Ouladdiaf, B.; Mandal, P.; Ghosh, B., *Phys. Rev. B* **2003**, *68*, 052406.
- (39) Ahmed, M. R.; Gehring, G. A., *Phys. Rev. B* **2009**, *79*, 174106.
- (40) Li, W.; Thirumurugan, A.; Barton, P. T.; Lin, Z.; Henke, S.; Yeung, H. H.-M.; Wharmby, M. T.; Bithell, E. G.; Howard, C. J.; Cheetham, A. K., *J. Am. Chem. Soc.* **2014**, *136*, 7801-8704.
- (41) Di Sante, D.; Stroppa, A.; Jain, P.; Picozzi, S., *J. Am. Chem. Soc.* **2013**, *135*, 18126-18130.
- (42) Shang, R.; Xu, G.-C.; Wang, Z.-M.; Gao, S., *Chem.-Eur. J.* **2014**, *20*, 1146-1158.
- (43) There is clear evidence of significant strain broadening in the diffraction patterns shown in Fig. 2(a) that appears to be more significant for compositions  $0.6 \leq x \leq 1$  ( $\text{Cd}^{2+}$  embedded in  $\text{Cu}^{2+}$  matrix) than  $0 \leq x \leq 0.4$  ( $\text{Cu}^{2+}$  embedded in  $\text{Cd}^{2+}$  matrix).
- (44) Whereas in conventional orbital order/disorder systems (e.g.  $\text{La}_{1-x}\text{Ca}_x\text{MnO}_3$ ) thermally-induced orbital reorganization is permitted via charge redistribution,<sup>49</sup> here it is likely that the distribution of JT-active cations is fixed during synthesis; hence the temperature-independence of  $x_0$ .
- (45) Shannon, R. D.; *Acta Cryst. A* **1976**, *32*, 751-767.
- (46) Paściak, M.; Welberry, T. R.; Kulda, J.; Kempa, M.; Hlinka, J., *Phys. Rev. B* **2012**, *85*, 224109.
- (47) Kieslich, G.; Kumagai, S.; Forse, A. C.; Sun, S.; Henke, S.; Yamashita, M.; Grey, C. P.; Cheetham, A. K., *Chem. Sci.* **2016**, *in press*; doi: 10.1039/C6SC01247G.
- (48) Chen, S.; Shang, R.; Wang, B.-W.; Wang, Z.-M.; Gao, S., *Angew. Chem. Int. Ed.* **2015**, *54*, 11093-11096.
- (49) Rao, C. N. R.; Cheetham, A. K., *Science* **1996**, *272*, 369-370.



$[\text{C}(\text{NH}_2)_3]\text{Cd}(\text{HCOO})_3$   
R-type multipole order



$[\text{C}(\text{NH}_2)_3]\text{Cu}(\text{HCOO})_3$   
O-type multipole order